Acoustic properties of coral sands, Waikiki, Hawaii

S. S. Fu
Hawaii Institute of Geophysics & Planetology, University of Hawaii, Honolulu, Hawaii 96822

C. Tao
Zhejiang University, Hang Zhou, 310027, China
Second Institute of Oceanography, Hang Zhou, 310012, China

M. Prasad
Department of Geophysics, Stanford University, Stanford, California 94305

R. H. Wilkens[a)]
Hawaii Institute of Geophysics & Planetology, University of Hawaii, Honolulu, Hawaii 96822

L. N. Frazer
Department of Geology & Geophysics, University of Hawaii, Honolulu, Hawaii 96822

(Received 8 May 2003; revised 18 December 2003; accepted 1 February 2004)

An *in situ* experimental study of variations of compressional wave speed and attenuation with depth in natural coral sands has been made offshore of Oahu, Hawaii. *In situ* data were collected at a center frequency of 7.5 kHz. Compressional wave speed averages around 1620 m/s and attenuation (expressed as Q_p^{-1}, the reciprocal of the quality factor) decreases from 0.04 at the seafloor to 0.01 at 2 m depth. Very little change in compressional wave speed is seen to 9 m below the seafloor. Coral sand sound speeds are lower than those reported elsewhere for quartz sand. Waveforms recorded over the upper 9 m below the seafloor exhibit virtually no peak broadening, suggesting that scattering contributes little to the *in situ* attenuation. The relationship of attenuation to frequency in the coral sands agrees with Hamilton's observations of attenuation in other sediments, although the coral sand attenuation is slightly higher than in other sediments. The coral sand relationship between attenuation and porosity also agrees with Hamilton's when the volume of intraparticle voids is deducted from the total porosity.
[DOI: 10.1121/1.1689340]

PACS numbers: 43.30.Ma [RAS] Pages: 2013–2020

I. INTRODUCTION

The geoacoustic properties of unconsolidated seafloor sediments are important factors controlling seismoacoustic propagation in the ocean. Complications arising from the variety of sediments, together with their depth and spatial variability, have presented a challenge to our understanding of acoustic behavior in marine sediments, especially in shallow water. In this study, we present the first *in situ* acoustic data from coral sand at subbottom depths greater than a few 10's of centimeters.

Coral sand deposits derived from active reefs constitute the dominant sediment cover on many modern shelves located at low latitudes in shallow, tropical to subtropical seas. They are almost ubiquitous in the many islands and atolls of the equatorial Pacific ocean. Despite the importance of coral sands in shallow water acoustics, the depth dependence of acoustic properties in natural coral sands is poorly known. Reasons for this include difficulties in coring, the usual difficulties of *in situ* measurement, and the complicated microstructure of coral sands.

We have developed an instrument, the acoustic lance, to obtain *in situ* compressional wave speed and attenuation profiles within the upper several meters of the seafloor (Fu *et al.*, 1996). This study reports lance measurements taken in a natural coral sand deposit, the Halekulani Sand Channel (HSC), off Waikiki on Oahu (Fig. 1).

Two sites were investigated in the HSC. At the first site, a 4 m long test probe deployment (Site 1 M1) was followed by a 9 m long probe deployment (Site 1 M2). At Site 2, two 2 m long probes were deployed 50 m apart (Site 2A, B). No cores were collected at Site 1, but six vibracores were recovered at Site 2 for laboratory study. We report *in situ* variations of compressional wave speed (V_p) and attenuation (Q_p^{-1}, the reciprocal of quality factor) with depth in the HSC and compare them with results of studies of quartz sands.

From *in situ* and laboratory core sample measurements, Hamilton (1980) obtained empirical relations between the acoustic and physical properties of many types of marine sediments. The parameters in those relations have been used successfully for decades to predict acoustic properties in different types of marine sediments. Lacking in Hamilton's coverage, however, were measurements from coral sand environments. Our observations of compressional wave speed between 0–10 m below the sea floor (mbsf) differ substantially from Hamilton's (1980) equation characterizing fine quartz sand.

To compare our attenuation results with the work of other investigators, Q_p^{-1} is converted to attenuation coeffi-

a)Corresponding author: Roy Wilkens;
electronic mail: rwilkens@Hawaii.edu; telephone: (808) 956-5228.

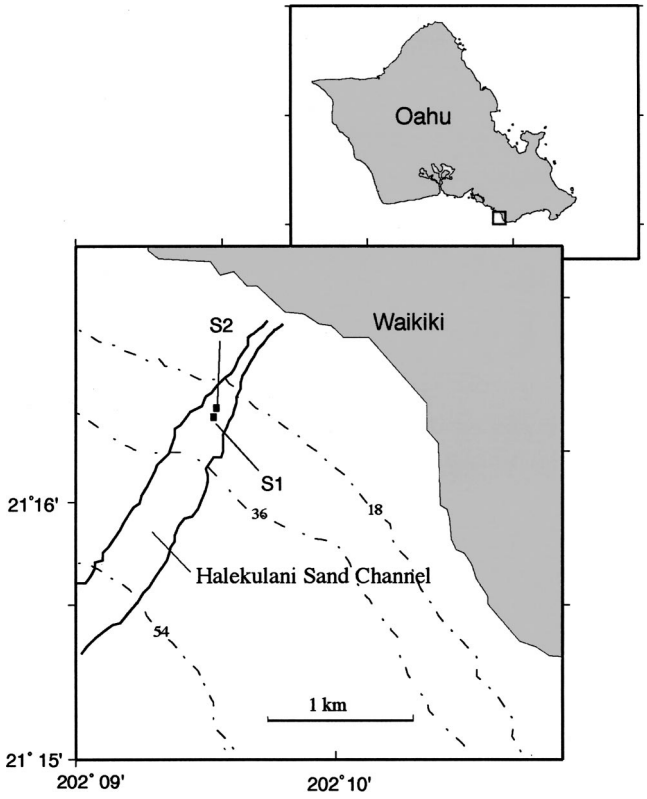

FIG. 1. Locations of acoustic lance deployment sites S1 and S2. Contour interval: 18 ft.

cients α and k. The attenuation data in coral sands agree with Hamilton's relationship between attenuation and porosity when the volume of intraparticle voids is deducted from the total porosity of the coral sands.

II. GEOLOGICAL SETTING

The Halekulani Sand Channel is located off the southern shore of the Hawaiian island of Oahu (Fig. 1). It extends from the shoreline to water depths greater than 30 m. The channel was probably part of an ancient stream drainage that was cut during a glacial low sea level stand. Sand transport in the HSC is affected by wave climate, as in the summer months when surf generated by Antarctic winter storms reaches the south shores of Oahu and reworks sands in water depths of up to 100 m. Hurricanes and tsunamis are infrequent, but their impact on sand transport is locally severe (Coulbourn *et al.*, 1988). This active environment results in a loose, poorly consolidated sediment comprising the upper 10's of meters of the sand deposits.

The HSC was chosen as the experiment site because it is a large, well-defined sand deposit. The sands show no indications of post-depositional cementation in the upper 10 m of the deposit and are poorly compacted. For this experiment, the physical parameters of the HSC sands—grain size, density, and porosity—were examined from core samples collected at the time of the experiment by Sea Engineering Inc. Samples show that the sediments within 0–8 mbsf in the channel are moderately well-sorted, greyish coral sands. A scanning electron microscope (SEM) backscattered electron image of a sample is shown in Fig. 2. The median grain size of the sand ranges from 0.19 to 0.38 mm (fine to medium sand). In general, silt and clay sizes comprise less than 10% of each sample by weight. A summary of sand characteristics in the HSC is presented in Table I. Because of wave related reworking of the sediments, there is no apparent relation between grain size and either spatial location of samples or depth of samples within the deposit.

Sediment analysis showed bulk density varying from 1.78 to 1.93 g/cm^3 and porosity varying from 0.49 to 0.57 in 39 core samples from the 6 cores recovered from the uppermost two meters of the HSC. However, the average bulk densities and porosities of each core are almost the same. Bulk densities averaged for each core are between 1.84 and 1.87 g/cm^3 and average porosities are between 0.52 and 0.54. Grain size distributions remain nearly constant in most of the samples, except for a small percentage of coral gravels present in some samples. These measurements suggest that the HSC sand deposit can be regarded as near-homogenous at meter scales (in the upper two meters), although at centimeter scales it may be inhomogeneous.

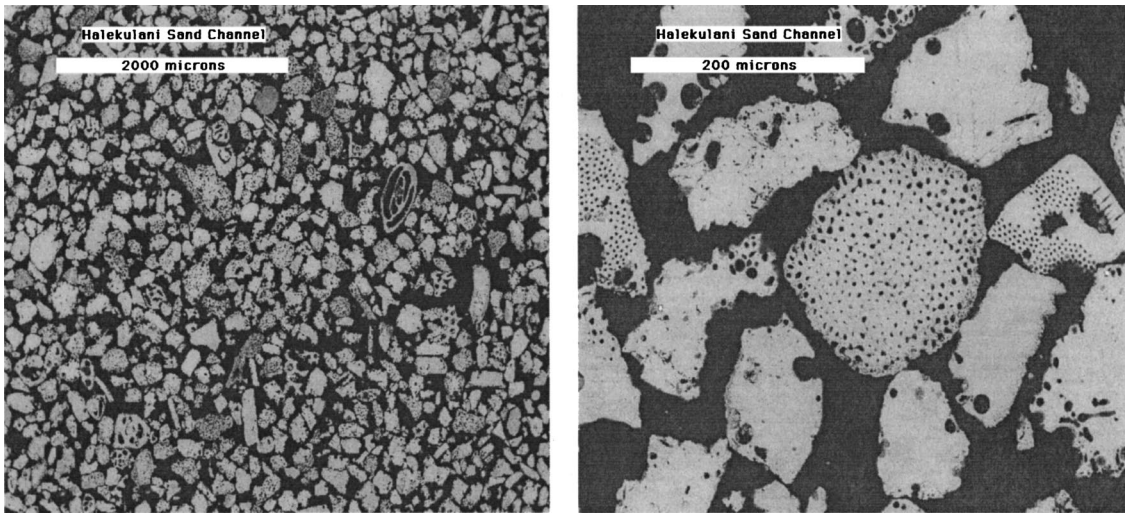

FIG. 2. Backscattered electron images of polished sections of coral sand from the Halekulani Sand Channel. Bright areas are calcium carbonate; dark areas are pore space.

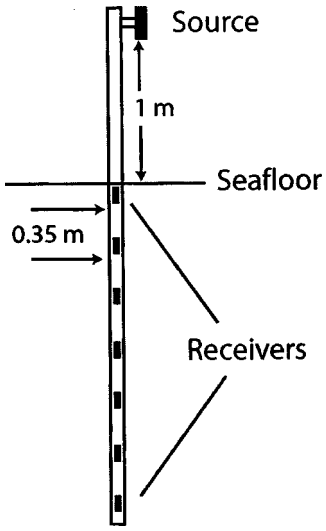

FIG. 3. Source and receiver geometry of the lance deployments at measurement Site 2. Not shown are the 2 receivers (1 m apart) above the source that were used to monitor bottom water sound speed.

III. METHODS

A. *In situ* measurement

The acoustic lance is a linear array of up to ten receivers embedded in the seafloor below an acoustic source (Fig. 3 and Fu *et al.*, 1996). It provides an *in situ* recording of full waveforms (Fig. 4) that travel vertically through the sediments. In deep-water operation a broadband acoustic source and a solid state data recording system are mounted on the weight stand of a gravity corer or an independent probe. An array of small hydrophones is mounted along the outside of the probe. In the HSC experiments, the receivers were mounted on a probe that was installed by using a water jet to penetrate the sands. After allowing a few days for sediment reconsolidation, divers brought the recording package down to the seafloor for measurements. The signal frequency band used in this analysis is 5–10 kHz, with the dominant frequency near 7.5 kHz. The spectrum of the top sediment receiver waveform in Fig. 4 is shown in Fig. 5 along with corrected spectra used for the attenuation calculation (see later).

The first deployment at the HSC (Site 1 M1) had three receivers mounted along a 4 m long probe at intervals of 2 m; all three receivers were buried in the coral sands. For the second deployment about 6 months later (Site 1 M2), 7 receivers were mounted along a 9 m subsurface probe at a spacing of 1.5 m; 2 receivers were positioned above the sediments to obtain the bottom water sound speed. The measurements were taken one week after the probe was inserted. The second deployment (Site 2A, B) was a more detailed study of acoustic structure in the upper 2 mbsf of the Halekulani sand channel. Lance measurements were made using two probes (A and B), each of which penetrated approximately two meters into the sediments; the horizontal distance between the two probes was about 50 m. Nine receivers were mounted on each probe. The top two receivers were in the water, 1 m apart, to obtain the bottom water sound speed while the remaining seven receivers penetrated the sediments at 0.35 m spacing. The first measurements were made with Probe A, two days after it was set up (Site 2A M1), and one week later a second set of measurements were made using Probe B (Site 2B M1). Two months later more data were collected from both probes (Site 2A, B M2).

Compressional wave speed (V_p) and attenuation (Q_p^{-1}) were extracted from the waveform recordings. Sound speed was estimated from the differences in signal arrival time at receivers of known separation. Errors or uncertainties in the calculations are a function of receiver spacing and the signal sampling rate (100 kHz). By interpolating the wave forms in the frequency domain, we increased the effective resolution of travel time to 2.5 μs. At a receiver separation of 35 cm (Site 2) this translates to 18 m/s in the sand—or roughly 1% of the average speed of 1620 m/s. At a separation of 1.5 m, the error is proportionally lower because the overall travel time is greater but the arrival uncertainty is constant. A complete discussion of errors and uncertainties in sound speed calculation from acoustic lance data can be found in Fu *et al.* (1996).

Effective attenuation, as it contains the effects of both intrinsic attenuation and scattering attenuation, is much more difficult to extract than sound speed, because whole wave forms must be used. Noise contamination and the correction for receiver transfer functions complicate signal processing, making a careful treatment of errors important. We corrected wave form spectra in the sediments for differences in receiver performance and for geometrical spreading by normalizing them with spectra recorded in water from the same receivers (Fig. 5). Frazer *et al.* (1999) describe in detail the two-step process used to extract attenuation (Q^{-1}) from the lance signals by an application of geophysical inverse theory to the spectral ratio method: In the first step, for every possible source–receiver interval the joint probability density function (pdf) of attenuation (effectively, spectral ratio slope)

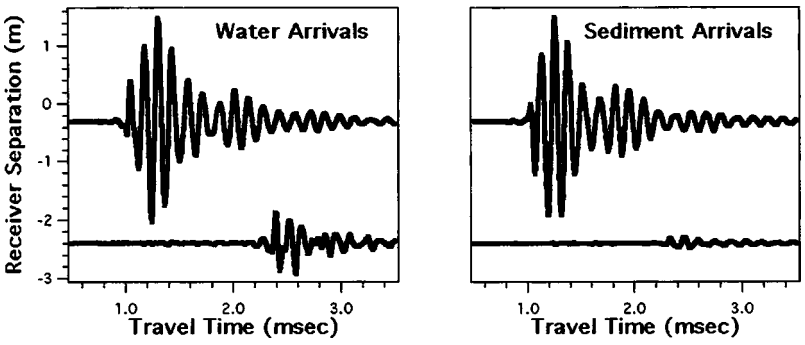

FIG. 4. Wave forms recorded by the top and bottom receivers of one of the Site 2 probes both in water (for calibration) and in the sediment. The receivers are separated by 210 cm. In each case the waveforms are normalized to the top receiver. The difference between the amplitudes of the top and bottom receivers in water (left panel) is essentially due to geometrical spreading. The greater difference in amplitudes seen in the sediment arrivals (right panel) is the result of effective attenuation.

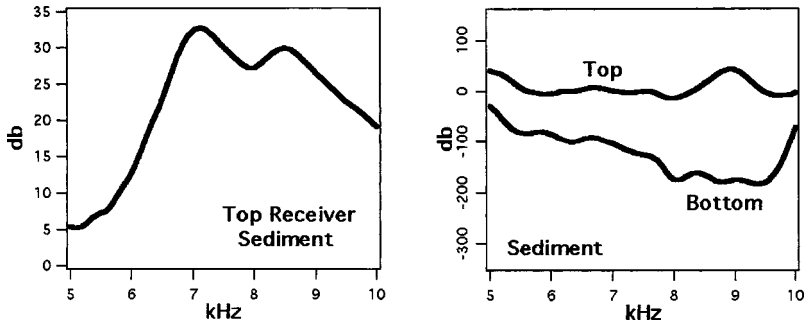

FIG. 5. Left—Spectrum of top sediment receiver waveform shown in Fig. 4. Right—Spectra for top and bottom sediment receivers shown in Fig. 4 corrected by dividing the spectra of the sediment arrivals by the spectra of the water arrivals. The difference in the slopes of these two spectra is used to calculate attenuation.

and the intercept is taken to be an L1 likelihood; a numerical integration over intercept then gives the marginal pdf of attenuation for that interval. In the second step, the peaks of these marginal pdfs are used as the data, and the half-widths of the marginal pdfs are used as the errors in an L1 likelihood taken to be the pdf of attenuation profiles. (The profile space has dimension equal to the number of receivers minus one.) Then the marginal pdf of the attenuation of each receiver–receiver (R–R) interval is obtained by numerically integrating the profile pdf over the attenuations of all other R–R intervals. A best profile is defined as the profile that agrees with the peak of the marginal pdf for each R–R interval. For brevity in this paper the marginal distributions are not shown; instead the attenuation profile uncertainty is indicated simply by plotting the envelope of the ten most probable profiles.

B. Analysis of core samples

The core samples in the HSC were collected by a vibracorer. The vibracorer uses motor-driven, counter-rotating vibrators attached to a 10 cm inner diameter, 3 m long core barrel. Samples analyzed in the laboratory were partially dry and had to be saturated with sea water under vacuum before making bulk density and porosity measurements. Vibracoring almost certainly disturbs the sediments it collects, and measurements of the porosity of core samples must be considered to be maximums. However, it must also be remembered that the HSC is located in an active wave climate and that these sands are naturally disturbed and transported repeatedly over the course of time. Thus we believe, although we cannot demonstrate, that the measured bulk properties are generally near *in situ* values.

Six samples were saturated with low viscosity epoxy, cut, polished, and examined using a scanning electron microscope (Fig. 2). Image processing of three views of each sample, at two magnifications each, was carried out to quantify the distribution of pore space between intertest and intratest pores. We used the NIH Image software package for image analysis. Pixels were first classified as either grain or pore (essentially black or white). Next, using a series of dilations followed by an equal number of erosions, the small intratest pores were removed from the image. Pixels were again classified as either pore or grain. The difference in the number of pore pixels before and after processing yielded the proportion of intratest pores—about 5% of the total, $\pm 0.5\%$. Tribble and Wilkens (1994) give a fuller description of the method, with examples.

IV. RESULTS

Waveforms recorded by the deepest probe (Site 1 M2) in the coral sands of the HSC are displayed in Fig. 6. The *in situ* compressional wave speed interval profiles from Site 1 (Fig. 7, Table II) show a speed of approximately 1595 m/s within the upper 4 m of the seafloor. The deep profile shows compressional wave speed generally increasing with depth, although that increase is not constant. Speed averages near 1600 m/s in the interval from 6.0 to 7.5 mbsf, while sound speeds above and below increase to around 1640 m/s. The long probe unfortunately could not be retrieved from the sediments for receiver transfer function calibration, which must be conducted in water (Frazer *et al.*, 1999); therefore no *in situ* attenuation data could be calculated from waveforms collected at Site 1.

It is noteworthy that little or no apparent signal broadening is seen in the self-normalized signals (Fig. 6). These wave forms are typical HSC measurements and they suggest that there is little scattering *in situ*, since scattering tends to redistribute energy from the signal onset to the coda. Thus our *in situ* attenuation calculations represent predominantly intrinsic losses.

The results of Site 2 experiments are given in Tables II and III and plotted in Figs. 8 and 9. Some of the waveforms had low signal/noise ratios due to failed receivers or to problems in recording; these waveforms were not used in subse-

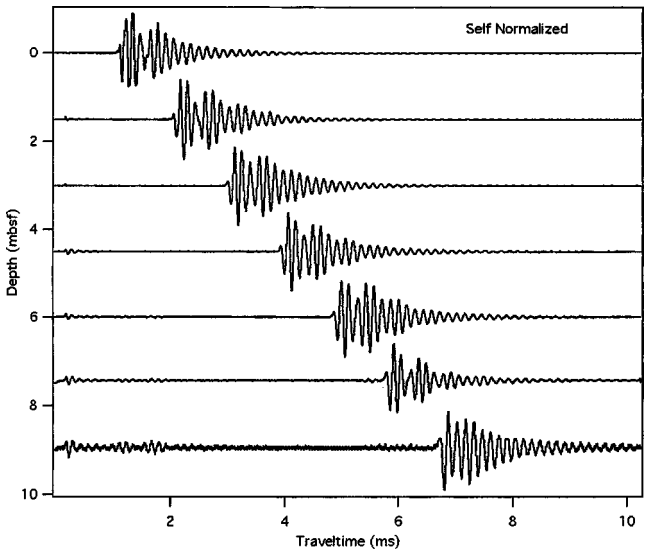

FIG. 6. Self-normalized full wave forms recorded by the acoustic lance in the Halekulani Sand Channel. Note that there is very little evidence of scattered energy arriving later in time in the more distant receivers.

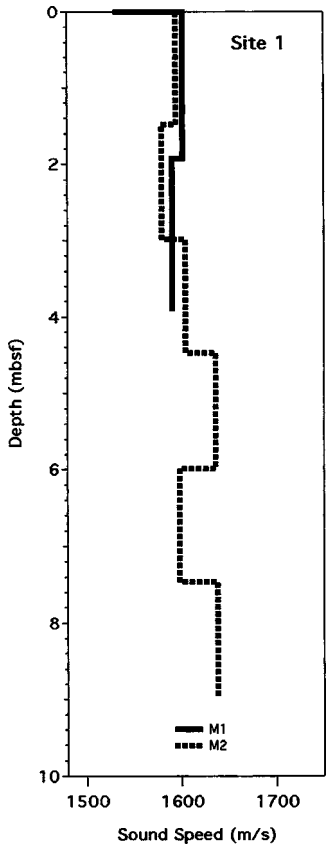

FIG. 7. *In situ* interval profiles of compressional wave speed measured at Site 1.

quent processing. At Site 2 (Fig. 8), the later measurements show some difference in compressional wave speed when compared to the measurements made two months earlier: the maximum disparity at the same depth is about 60 m/s, which is more than the expected measurement error of 1%. However, the speed inhomogeneity at the 0.35 m scale is not seen when data are averaged over 2 m. At Probes A and B the average compressional wave speeds during the second measurement over the entire 0–2 mbsf interval are virtually identical: 1631 m/s at Probe A and 1632 m/s at Probe B. The speed disparity between repeat measurements is largest at Probe A, perhaps because of sediment disturbance by the water jet. This conjecture is supported by the fact that where there are differences the later measurements are generally faster than the earlier measurements. The first measurement at Probe A was conducted only two days after it was installed, and the sediments, disturbed by the water jet, may not have completely reconsolidated in this short time. The average interval sound speeds (M1 and M2) at each of the two probes do not show an increase with depth, although interval speed varies more at Probe A than at Probe B, where it is nearly constant.

TABLE I. Summary of HSC sand characteristics.

Average median grain size	0.21 mm
Range of median grain sizes	0.19–0.25 mm
Sorting	Well sorted
Grain density	2.82 g/cm^3
Porosity average	0.53
Porosity range	0.49–0.57

TABLE II. Summary of *in situ* sound speed.

Site 1 M1		Site 1 M2	
Depth (m)	*Vp* (m/s)	Depth (m)	*Vp* (m/s)
0–1.9	1601	0–1.5	1594
1.9–3.9	1590	1.5–3.0	1579
		3.0–4.5	1604
		4.5–6.0	1636
		6.0–7.5	1598
		7.5–9.0	1638
Site 2A M1		Site 2A M2	
0–0.35	1613	0–0.35	1639
0.35–0.69	1602	0.35–0.69	1602
0.69–1.00	1672	0.69–1.00	1653
1.00–1.37	1608	1.00–1.37	1660
1.37–1.72	1613	1.37–1.72	1666
1.72–2.07	1626	1.72–2.07	1595
Site 2B M1		Site 2B M2	
0–0.68	1637	0–0.34	1602
0.68–1.37	1636	0.34–0.68	1647
1.37–1.72	1639	0.68–1.37	1636
1.72–2.07	1601	1.37–1.72	1626
		1.72–2.07	1659

Accurate laboratory measurements of attenuation at sonic frequencies (typically 1–20 kHz) are greatly limited by the sample length (the sample length must be several times larger than a wavelength). This difficulty may be addressed by performing attenuation measurements *in situ*, as with the lance. Attenuation measured from field data is termed an effective attenuation, because it includes both intrinsic and scattering attenuation. When scattering is small, as in our case, effective attenuation is approximately equal to intrinsic attenuation.

The envelopes of the ten most probable attenuation profiles for measurements 1 and 2 at Probe A and for measurement 2 at Probe B are shown in Fig. 9. For Probe B several of the wave forms recorded during the first measurement were too noisy for reliable attenuation calculations, although sound speed picks were possible. Accordingly, we show only one attenuation profile for Site 2B (Fig. 9, right panel). All three profiles show a decrease in attenuation with depth. This is most likely an effect of overburden pressure. There are three possible mechanisms for attenuation relevant to *in situ* data. One mechanism is the squirt of fluid through the solid matrix in response to deformation (Stoll, 1985; Kibblewhite, 1989). However, squirt is usually significant in high permeability solids such as sands only at low frequencies (1–1000 Hz) (Kibblewhite, 1989; Hamilton, 1980). A second possible

TABLE III. *In situ* attenuation (Q^{-1}) measurements.

Probe A	M1	M2	Probe B	Combined
Depth (m)	Q^{-1}	Q^{-1}	Depth (m)	Q^{-1}
0.00–0.69	$\geqslant$0.05	0.045	0.00–0.68	$\geqslant$0.05
0.69–1.00	$\geqslant$0.05	$\geqslant$0.05	0.68–1.37	0.025
1.00–1.37	$\leqslant$0.01	0.036	1.37–1.72	0.020
1.32–2.07	$\leqslant$0.01	0.022	1.72–2.07	$\leqslant$0.005

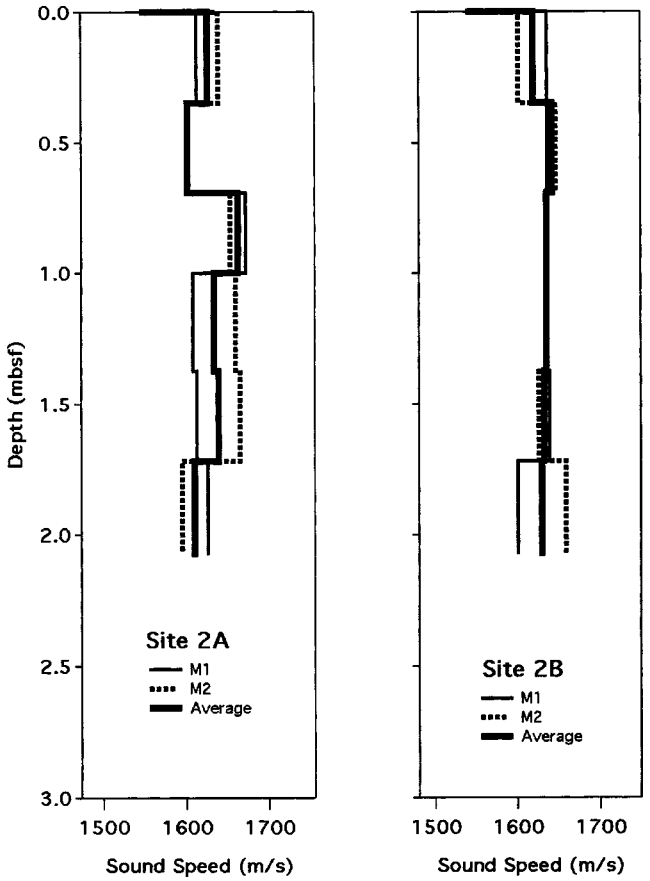

FIG. 8. *In situ* interval profiles of compressional wave speed measured at Site 2.

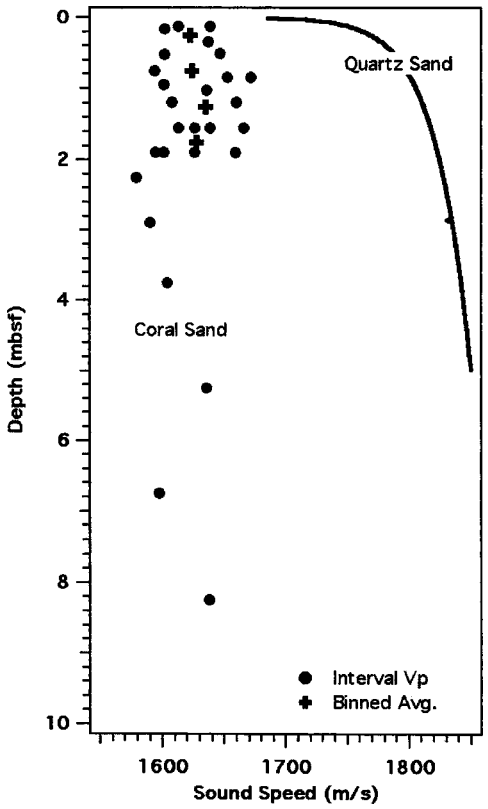

FIG. 10. *In situ* coral sand sound speed and quartz sand curve from Hamilton (1980). Points represent the middle of each measurement interval. Crosses are binned averages of all of the 2 m long probe data.

cause of attenuation is scattering due to heterogeneity such as lumps or layers. This kind of attenuation generally moves energy from the onset of the wave into the coda, a phenomenon not seen in our *in situ* data. A third possible cause of attenuation is grain boundary sliding (Stoll, 1985; Kibblewhite, 1989; Hamilton, 1972) related to low levels of compressive loading, as when contact stiffness of grains increases in deeper sediments, attenuation decreases with depth.

V. DISCUSSION

Interval sound speed data, plotted at the midpoint of each depth interval, binned averages of the shallower data, and Hamilton's (1980) empirical equation for fine quartz sand are plotted in Fig. 10. It is apparent that our *in situ* measurements do not fit speed-depth profiles for sand that are in the literature. This may well reflect the fact that much of the earlier work was based on studies of continental shelf-type quartz sands (e.g. Hamilton, 1980). Both the coral sands and the quartz sands exhibit very little increase in speed with depth over the upper 10 mbsf, but the coral sands are significantly slower than their quartz counterparts. A study of near-surface (0.05–0.30 mbsf) *in situ* compressional wave speed in carbonate sediments of the Dry Tortugas (Richardson *et al.*, 1997) yielded results generally in the same speed range as our HSC observations.

Hamilton (1976) analyzed the attenuation of compres-

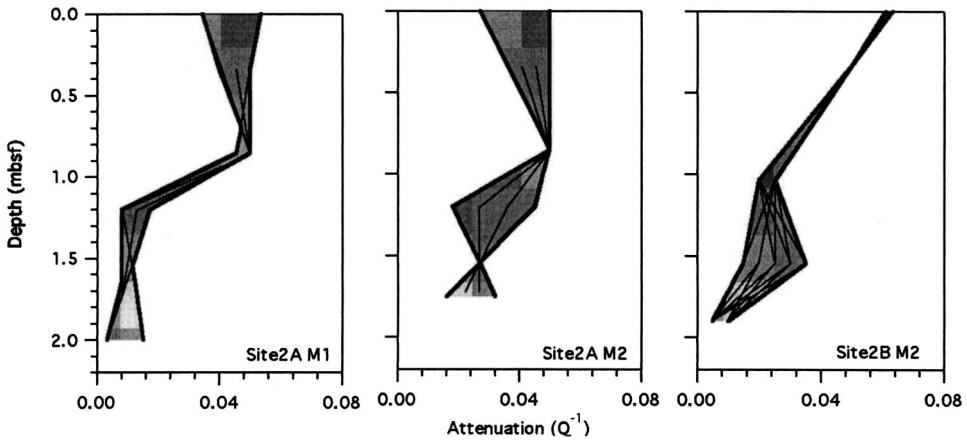

FIG. 9. *In situ* attenuation profiles from Probes A and B at Site 2. Each shaded zone is the envelope of the ten most probable profiles.

sional waves versus depth in the seafloor from various reported data at a range of frequencies. Hamilton's results were given in terms of the parameter k, which comes from the amplitude relation for an attenuating plane wave in the form

$$10\log\left|\frac{A^2(x_2)}{A^2(x_1)}\right| = -kf(x_2 - x_1), \tag{1}$$

where x_1 and x_2 are source–receiver distances, k is in dB/m kHz, and f is frequency in kHz. The relation between k and the other commonly used measures of attenuation is

$$\alpha = kf = \frac{20\pi f}{\ln(10)}\frac{1}{Qc} = \frac{8.686\pi f}{Qc}, \tag{2}$$

where α is in dB/m, c is wave speed, and the quality factor Q is dimensionless. Referring to the results of Gardner *et al.* (1964) and Hunter *et al.* (1961) on the relationship of attenuation to pressure in sands, Hamilton assumed a decrease of k with the $-1/6$ power of depth (overburden pressure) in sandy sediments. With this assumption, he computed attenuation versus depth from k values measured in surficial sediments. The results showed that, in fine sands, attenuation decreases rapidly with increasing depth to about 10 m, and then decreases less rapidly to 150 m. Our *in situ* attenuation profiles (Fig. 9) agree with Hamilton's description. Attenuation decreases rapidly in the upper 2 m interval of the HSC coral sands. Our data provide new evidence that in sandy deposits the maximum attenuation variation may take place in the uppermost several meters of the seafloor while speed itself may remain fairly constant.

Next we compare our *in situ* attenuation data for the HSC coral sand with Hamilton's (1972, 1976) regression for attenuation versus porosity, shown in Fig. 11. To minimize the experimental errors and the effects of local inhomogeneity, average attenuation values were calculated for the measurements. Our averaging scheme for *in situ* attenuation weights longer travel times—see Eqs. (6) and (24) of Frazer *et al.* (1999). The final average attenuation of the entire upper 2 m interval was taken as the mean of the three profiles ($Q^{-1} = 0.032, k = 0.53$ db/m kHz). In his regression, Hamilton used data for a variety of sediments, including clays, silts, and sands, although no pure coral sands were among these sediments. The data show that the sensitivity of attenuation to porosity varies greatly between porosities of 0.47 and 0.65 (medium sands to silt–clay). Within this porosity range, k changes from 0.52 to 0.77, then drops to 0.12. We have added an averaged *in situ* attenuation constant ($k = 0.53$) and the averaged total porosity in the HSC coral sands to Hamilton's plot as well as the sand data from Hamilton (1972) (Fig. 11). Our raw data lie on the lower boundary of Hamilton's data distribution; it seems that either k or porosity is too low for the Hamilton attenuation-porosity curves to be good predictors of attenuation in coral sand. However, total porosity includes both intraparticle and interparticle voids. Most likely, the poor agreement results from the presence of intraparticle voids in coral sands which are counted in total porosity but have little effect on the grain-to-grain contact area, a dominant factor controlling sound

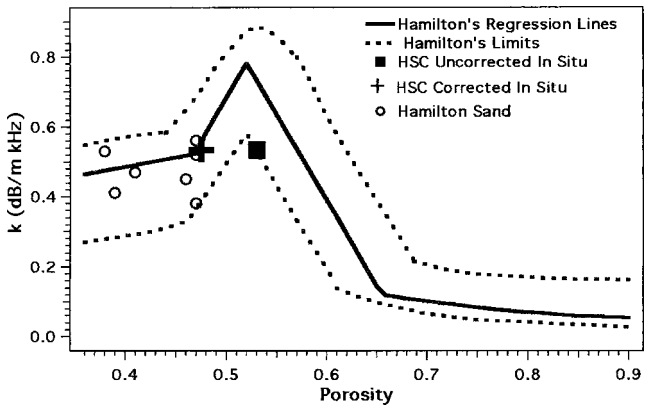

FIG. 11. Hamilton's (1976) regression lines for attenuation versus porosity. HSC *in situ* data and Hamilton's sand measurements are added to the plot. The corrected value has intragrain porosity removed.

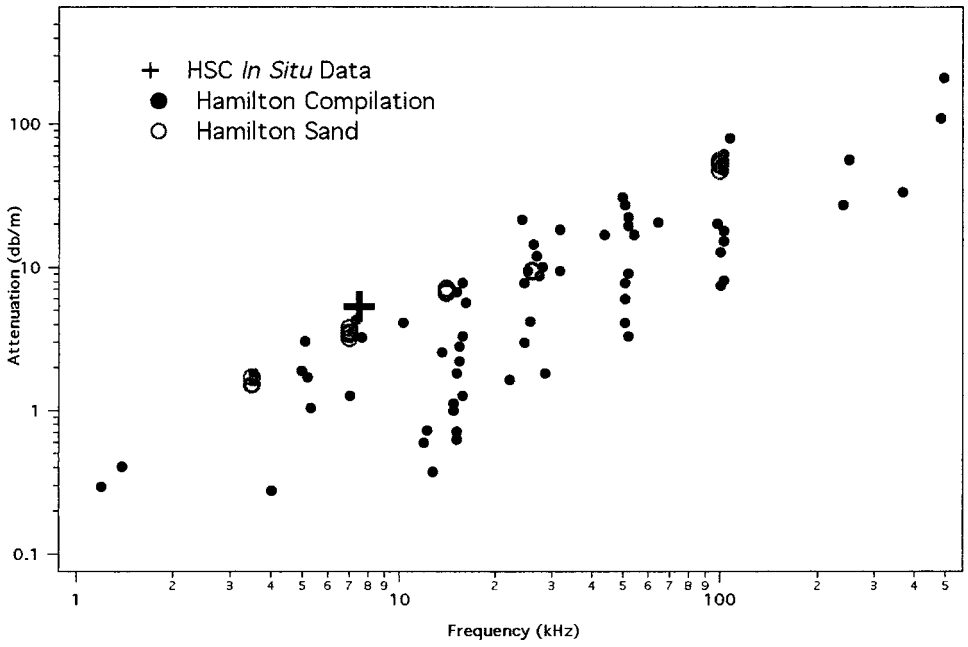

FIG. 12. Attenuation versus frequency after Hamilton (1980). Data have been added from this study and Hamilton's sand measurements have been highlighted.

wave transmission in sands (Digby, 1981; Hamilton, 1972). The results of our image processing showed that intraparticle voids occupy about 5% of the total sample volume. When the volume of intraparticle voids is deducted from total porosity, our average attenuation measurement matches Hamilton's equation well (Fig. 11). It suggests that, as Hamilton (1982) pointed out, hollow grains act as solid particles in transmitting sound waves. Because attenuation is sensitive to porosity in the sediments from medium sands to silt–clays (porosity of 0.47–0.65), our data show that caution must be exercised when using bulk porosity as an index property to predict attenuation in coral sands.

In situ attenuation is plotted in Fig. 12 as attenuation coefficient along with the data from Hamilton's (1980) compilation of all sediments. Hamilton's (1972) data are also highlighted in the plot. These coral sand average falls along the upper edge of the of the Hamilton data compilation, although it is not much greater than Hamilton's (1972) measurements made at 7 kHz.

VI. CONCLUSIONS

We have presented the first *in situ* measurements of acoustic properties in coral sand beyond a few decimeters below the seafloor. Compressional sound speeds are lower than those published in the literature for quartz sands. Attenuation is severe—some of the highest values measured in marine sediments—and decreases with depth within the upper 2 m of the seafloor. The quality of the waveforms suggests that there is very little scattering within the sediments tested, and that the attenuation measured is primarily intrinsic. Our *in situ* attenuation data agree with Hamilton's relation of attenuation to porosity if the volume of intraparticle voids is deducted from total porosity.

ACKNOWLEDGMENTS

This work was supported by the Office of Naval Research Ocean Acoustics Program, by Grant No. NSFC49906004 from the National Science Foundation of China, Grant No. 2000502 from State Oceanography Administration and Grant No. 2002AA615130 from the Hi-Tech Research and Development Program of China. We also thank the staff of Sea Engineering, Inc. for allowing us to piggyback on their survey of offshore sand deposits on Oahu.

Coulbourn, W. T., Campbell, J. F., Anderson, P. N., Daugherty, P. M., Greenberg, V. A., Izuka, S. K., Lauritzen, R. A., Tsutsui, B. O., and Yan, C. (**1988**). ''Sand deposits offshore Oahu, Hawaii,'' Paci. Sci. **42**, 267–299.

Digby, P. J. (**1981**). ''The effective elastic moduli of porous granular rocks,'' J. Appl. Mech. **48**, 803–808.

Frazer, L. N., Fu, S. S., and Wilkens, R. H. (**1999**). ''Seabed sediment attenuation profiles from a movable subbottom acoustic vertical array,'' J. Acoust. Soc. Am. **106**, 120–130.

Fu, S. S., Wilkens, R. H., and Frazer, L. N. (**1996**). ''Acoustic lance: New *in situ* seafloor velocity profiles,'' J. Acoust. Soc. Am. **99**, 234–242.

Gardner, G. H. F., Wyllie, M. R. J., and Droschak, D. M. (**1964**). ''Effects of pressure and fluid saturation on the attenuation of elastic waves in sands,'' J. Pet. Technol. **16**, 189–198.

Hamilton, E. L. (**1982**). ''Sound velocity and related properties of marine sediments,'' J. Acoust. Soc. Am. **72**, 1891–1904.

Hamilton, E. L. (**1980**). ''Geoacoustic modeling of the sea floor,'' J. Acoust. Soc. Am. **68**, 1313–1340.

Hamilton, E. L. (**1976**). ''Sound attenuation as a function of depth in the sea floor,'' J. Acoust. Soc. Am. **59**, 528–535.

Hamilton, E. L. (**1972**). ''Compressional-wave attenuation in marine sediments,'' Geophysics **37**, 620–646.

Hunter, A. N., Legge, R., and Matsukawa, E. (**1961**). ''Measurements of acoustic attenuation and velocity in sand,'' Acustica **11**, 26–31.

Kibblewhite, A. C. (**1989**). ''Attenuation of sound in marine sediments: A review with emphasis on new low-frequency data,'' J. Acoust. Soc. Am. **86**, 716–738.

Richardson, M. D., Lavoie, D. L., and Briggs, K. B. (**1997**). ''Geoacoustic and physical properties of carbonate sediments of the lower Florida Keys,'' Geo-Mar. Lett. **17**, 316–324.

Stoll, R. D. (**1985**). ''Marine sediment acoustics,'' J. Acoust. Soc. Am. **77**, 1789–1799.

Tribble, J. S., and Wilkens, R. H. (**1994**). ''Microfabric of altered ash layers, ODP Leg 131, Nankai Trough,'' Clays Clay Miner. **42**, 428–436.